Ultraviolet-B Protective Effect of Flavonoids from *Eugenia caryophylata* on Human Dermal Fibroblast Cells

Juilee Patwardhan, Purvi Bhatt

Department of Biological Sciences, Sunandan Divatia School of Science, SVKM's NMIMS (Deemed to be) University, Mumbai - 400 056, Maharashtra, India

ABSTRACT

Background: The exposure of skin to ultraviolet-B (UV-B) radiations leads to deoxyribonucleic acid (DNA) damage and can induce production of free radicals which imbalance the redox status of the cell and lead to increased oxidative stress. Clove has been traditionally used for its analgesic, anti-inflammatory, anti-microbial, anti-viral, and antiseptic effects. **Objective:** To evaluate the UV-B protective activity of flavonoids from *Eugenia caryophylata* (clove) buds on human dermal fibroblast cells. **Materials and Methods:** Protective ability of flavonoid-enriched (FE) fraction of clove was studied against UV-B induced cytotoxicity, anti-oxidant regulation, oxidative DNA damage, intracellular reactive oxygen species (ROS) generation, apoptotic morphological changes, and regulation of heme oxygenase-1 (HO-1) gene through nuclear factor E2-related factor 2 antioxidant response element (Nrf2 ARE) pathway. **Results:** FE fraction showed a significant antioxidant potential. Pretreatment of cells with FE fraction (10–40 µg/ml) reversed the effects of UV-B induced cytotoxicity, depletion of endogenous enzymatic antioxidants, oxidative DNA damage, intracellular ROS production, apoptotic changes, and overexpression of Nrf2 and HO-1. **Conclusion:** The present study demonstrated for the first time that the FE fraction from clove could confer UV-B protection probably through the Nrf2-ARE pathway, which included the down-regulation of Nrf2 and HO-1. These findings suggested that the flavonoids from clove could potentially be considered as UV-B protectants and can be explored further for its topical application to the area of the skin requiring protection.

Key words: Anti-oxidants, *Eugenia caryophylata*, human dermal fibroblasts, oxidative stress, ultraviolet radiations

SUMMARY

- Pretreatment of human dermal fibroblast with flavonoid-enriched fraction of *Eugenia caryophylata* attenuated effects of ultraviolet-B radiations
- It also conferred protection through nuclear factor E2-related factor 2-antioxidant response pathway and increased tolerance of cells against oxidative stress
- Flavonoid-enriched fraction can be explored further for topical application to the skin as a ultraviolet-B protectant.

Abbreviations used: ABTS: 2,2'-azino-bis-(3-ethylbenzothiazoline- 6-sulphonic acid), AO: Acridine orange, ANOVA: Analysis of variance, ARE: Antioxidant response elements, BSA: Bovine serum albumin, CAPE: Caffeic acid phenethyl ester, CAT: Catalase, DCFH-DA: 2',7'-dichlorofluorescein diacetate, DMEM: Dulbecco's Modified Eagle's Medium, DMSO: Dimethyl sulfoxide, DNA: Deoxyribonucleic acid, DPBS: Dulbecco's phosphate buffered saline, DPPH: 2,2-diphenyl-1-picrylhydrazyl, ECL: Enhanced chemiluminescence, EDTA: Ethylenediaminetetraacetic acid, ELISA: Enzyme-linked immunesorbent assay, EtBr: Ethidium bromide, FBS: Fetal bovine serum, FE fraction: Flavonoid-enriched fraction, FRAP: Ferric reducing antioxidant power, GPx: Glutathione peroxidase, GR: Glutathione reductase, GST: Glutathione-S-transferase, GSH: Reduced glutathione, GSSG: Oxidized glutathione, HDF: Human dermal fibroblast, HEPES: 4-(2-hydroxyethyl)-1-piperazineethanesulphonic acid, HRP: Horseradish peroxidase, HO-1: Heme oxygenase-1, HPTLC: High-performance thin layer chromatography, Keap-1: Kelch-like ECH-associated protein-1, MTT: 3-(4,5-dimethylthiazol-2-yl)-2,5-diphenyltetrazolium bromide, NaCl: Sodium chloride, NFDM: Nonfat dry milk, Nrf2: Nuclear factor E2-related factor 2, NQO1: NAD (P) H: Quinine oxidoreductase 1, OH: Hydroxyl ions, PBST: Phosphate buffered saline with 0.1% tween 20, PCR: Polymerase chain reaction, PMSF: Phenylmethanesulfonyl fluoride, Rf: Retention factor, ROS: Reactive oxygen species, rRNA: Ribosomal ribonucleic acid, SDS: Sodium dodecyl sulfate, SOD: Superoxide dismutase, TLC: Thin layer chromatography, TLC-DPPH: Thin layer chromatography-2,2-diphenyl-1-picrylhydrazyl, UV: Ultraviolet, UV-A: Ultraviolet-A, UV-B: Ultraviolet-B, UV-C: Ultraviolet-C, and qPCR: Quantitative polymerase chain reaction.
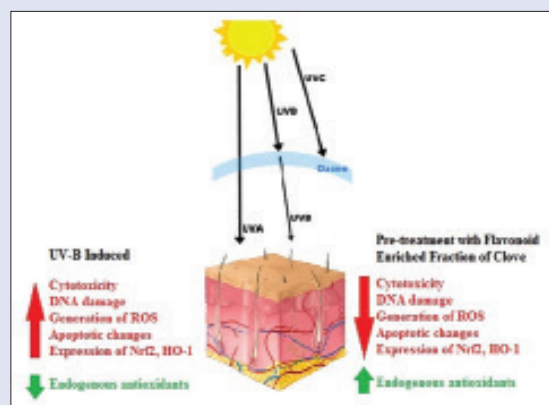
Correspondence:

Dr. Purvi Bhatt,
Department of Biological Sciences, Sunandan Divatia School of Science, SVKM's NMIMS (Deemed to be) University, Vile Parle (West), Mumbai - 400 056, Maharashtra, India.
E-mail: purvi.bhatt@nmims.edu
DOI : 10.4103/0973-1296.168979

INTRODUCTION

Skin is the largest organ of the human body acting as a barrier against various external insults including solar ultraviolet (UV) radiation. The UV spectrum is divided into three categories, UV-C (100–280 nm), UV-B (280–315 nm), and UV-A (315–400 nm). Out of the total solar UV radiation reaching the earth, 95% is UV-A, 5% is UV-B, and UV-C is totally absorbed by the ozone layer.[1,2] UV-B radiation is 1000 times more genotoxic than UV-A affecting the epidermal and dermal layer of the skin also producing various direct and indirect effects.[3] DNA

may absorb UV-B directly leading to mutations, the formation of cyclobutanepyrimidine dimers, photoproducts, etc., and p53 and its associated proteins may also induce apoptosis. UV-B induced mutations occurring in the p53 gene lead to a loss in the apoptosis control of the cell.[4] UV-B interacts with chromophores and photosensitizers indirectly generating free radicals which modify biomolecules such as proteins, lipids, and DNA.

When reactive oxygen species (ROS) levels exceed a threshold, the oxido-redox status of the cell is altered, and oxidative stress ensues. Hence, antioxidants are required to neutralize excess free radicals. Synthetic antioxidants and sunscreens are used for protection against free radicals and UV-induced damage, but they have limitations on continual use. Reports suggest that thymine dimer formation, induction of p53 and immunosuppression continue at suberythemal levels.[5] Photoaging leads to disarrangement of collagen, elastin, fibronectin, and proteoglycans in dermal layer whereas fibroblasts present in submucosal and subcutaneous tissues are required for repair of tissue injury.[3]

The human body has various defence systems against oxidative stress that are surpassed in extensive damage, one of which is the nuclear factor E2-related factor-2 antioxidant response element (Nrf2 ARE) pathway. The Nrf2 is a transcription factor bound to its inhibitor kelch-like ECH-associated protein-1 (Keap-1) that constantly ubiquitinates Nrf2 under normal metabolic conditions. During oxidative stress, the bond between Nrf2 and Keap-1 is lost and Nrf2 translocates into the nucleus where it binds to ARE present in the promoter regions of antioxidant enzyme genes such as heme oxygenase-1 (HO-1), glutathione-S-transferase, and NAD (P) H: Quinine oxidoreductase 1.[6-8] In the current study, we studied HO-1 gene regulation along with the protective effect of fraction though Nrf2-ARE pathway following UV-B irradiation. HO-1 enzyme converts heme into biliverdin that is converted to endogenous nonenzymatic antioxidant bilirubin.

Plant molecules such as polyphenols and flavonoids with antioxidant and free radical scavenging potential may be used as UV-B protectants. Antioxidants from natural sources are now applied topically as oral supplementation limits the amount reaching the skin due to biochemical processes.[4] *Eugenia caryophylata* (clove) possesses good antioxidant activity, high phenolic content[9] and used as analgesic, anti-inflammatory, anti-microbial, anti-viral, antiseptic agent, etc. The essential oils from clove are known to have a good antioxidant activity.[10,11] Clove contains a very high content of essential oil (20%) with Eugenol as a major constituent (60–95%)[12] along with high content of flavonoids and polyphenols which have potent pharmacological activities. Some compounds identified in clove are quercetin, kaempferol, luteolin, myricetin, gallic acid, ellagic acid, rhamnocitrin, and oleanolic acid.[10,11]

UV-B protective effect of various polyphenolic compounds such as silymarin,[13] sesamol,[3] ursolic acid,[14] ferulic acid, and[15] epicatechin gallate,[16] have been extensively studied. In the current study, protective activity of flavonoid-enriched (FE) fraction of clove has been studied against UV-B-induced oxidative damage in cultured human dermal fibroblast (HDF) cells by evaluating UV-B-induced cytotoxicity, intracellular ROS levels, endogenous enzymatic antioxidant levels, DNA damage, apoptotic changes, and HO-1 regulation through the Nrf2-ARE pathway.

MATERIALS AND METHODS

Chemicals

HDF (ATCC no. PCS-201-012) from Scientific Research Centre, V.G. Vaze College, Mumbai; Silica Gel 60 F$_{254}$ precoated plates, agarose, and goat

anti-mouse horseradish peroxidase (HRP)-conjugated secondary antibody from Merck (NJ, USA); Dulbecco's Modified Eagle's medium (DMEM), fetal bovine serum (FBS), penicillin-streptomycin, Dulbecco's phosphate buffered saline (DPBS), trypsin-ethylenediaminetetraacetic acid (EDTA), and 4-(2-hydroxyethyl)-1-piperazineethanesulphonic acid (HEPES) from Genetix Biotech (New Delhi, India); 2′,7′-dichlorofluorescein diacetate (DCFH-DA) dye, monoclonal antibodies against Nrf2 and HO-1 from Abcam (MA, USA); 3-(4,5-dimethylthiazol-2-yl)-2,5-diphenyltetrazolium bromide (MTT) from HiMedia Labs (Mumbai, India); ethidium bromide (EtBr) and acridine orange (AO) from SRL (Mumbai, India); natural product reagent, 2,2-diphenyl-1-picrylhydrazyl (DPPH), 2,2'-azino-bis-(3-ethylbenzothiazoline-6-sulphonic acid) (ABTS), monoclonal antibody against β-actin, TRI reagent, and silymarin from Sigma (St. Louis, MO, USA); cDNA synthesis kit from TAKARA (Shiga, Japan); primers for Nrf2 and HO-1 from Eurofins (Luxembourg, Germany); SYBR green real-time polymerase chain reaction (PCR) master mix from Roche (BASEL, Switzerland); horseradish peroxidase (ECL) substrate from Bio-Rad (Berkeley, California); X-ray films from Kodak (NY, USA); and protease inhibitor cocktail from Amresco (OH, USA). All other chemicals, solvents, and reagents were of analytical grade from S.D. Fine Chemicals (Mumbai, India) and Fisher Inorganic and Aromatic Limited (Mumbai, India).

Extraction and enrichment of flavonoids

The crude alcoholic extract was prepared by cold extraction technique using n-hexane, chloroform, and alcohol successively as previously reported.[17] Preliminary analysis showed the presence of flavonoids in the alcoholic extract, hence, it was used for enrichment of flavonoids.

Ten grams crude alcoholic extract was dissolved in 100 ml of distilled water and subjected to enrichment thrice using ethyl acetate.[18] The FE fractions were pooled, concentrated, and stored in vacuum until further use.

TLC, TLC-DPPH and HPTLC analysis

Thin layer chromatography (TLC) and TLC-DPPH analysis was performed for detection of flavonoids in the crude alcoholic extract and FE fraction using quercetin, kaempferol, and gallic acid standards. Silica Gel 60 F$_{254}$ precoated plates were used for analysis, and solvent system used was as previously described.[17] One percent Natural product reagent was used as derivatizing reagent and plates were observed under UV (366 nm) as previously reported.[17-19] Another derivatizing reagent used was 0.1% DPPH and plates were observed under visible light.[20] High-performance thin layer chromatography (HPTLC) was performed for the FE fraction using DESAGA HPTLC system. The chromatograms were scanned at 420 nm after derivatization with 1% natural product reagent. The spectra and retention factor (Rf) values were recorded using ProQuant software (Informer Technologies, Inc.).

Flavonoid content

Flavonoid content of FE fraction was estimated by the previously described method.[21] Quercetin was used as a standard in the concentration range of 10–100 μg/ml.

Anti oxidant activity by DPPH, ABTS and FRAP assay

The antioxidant potential of FE fraction was evaluated by DPPH, ABTS, and ferric reducing antioxidant power (FRAP) assays by

methods previously described[22-24] and was compared to crude alcoholic extract.[17]

FE fraction was studied further for UV-B protective activity in HDF cells.

Cell culture

HDF cells (ATCC no. PCS-201-012) were grown in DMEM supplemented with 10% FBS, 100 units/ml of penicillin, 0.1 mg/ml of streptomycin, and 2.5 μg/ml of amphotericin at 37°C, 5% CO_2.

Treatment groups

The HDF cells were divided into seven treatment groups as follows:
- Group 1: Control
- Group 2: FE fraction control (40 μg/ml fraction treated fibroblasts)
- Group 3: UV-B control (UV-B irradiated fibroblasts)
- Group 4: Positive control (UV-B irradiated fibroblasts + 5 μg/ml silymarin)
- Group 5: UV-B-irradiated fibroblasts + 10 μg/ml FE fraction
- Group 6: UV-B-irradiated fibroblasts + 20 μg/ml FE fraction
- Group 7: UV-B-irradiated fibroblasts + 40 μg/ml FE fraction.

Treatment of human dermal fibroblast cells

Cultured HDF cells were treated with FE fraction (Group 2, 5, 6, 7) and silymarin (group 4) 24 h prior to UV-B irradiation. Preliminary studies were done by MTT assay to ensure these concentrations were nontoxic. After fraction pretreatment, cells were washed with DPBS and covered with a minimum amount of serum-free DMEM.

Irradiation procedure

A UV-B tube (Sankyo Denki, Japan) served as a UV-B source with a wavelength range of 280–315 nm and peaked at 312 nm. The cells were irradiated at an intensity of 5 mW/cm² for 500 s with total UV-B radiation of 2.5 J/cm² showing 50% cell viability. After irradiation, cells were incubated at room temperature for 30 min, washed with DPBS, and studied further.

Cytoprotection by MTT assay

HDF cells (5×10^4) were seeded in 96 well plates followed by the pretreatment of FE fraction and silymarin. After 24 h, cells were washed with DPBS and then UV-B irradiated. Cells were incubated at room temperature for 30 min followed by MTT (5 mg/ml) addition and incubation at 37°C for 4 h. 150 μl dimethyl sulphoxide was added to each well and absorbance was read on enzyme-linked immune sorbent assay reader at 570 nm.[25]

Estimation of endogenous antioxidants

Cell lysates were prepared from treatment groups using a lysis buffer containing 50 mM tris-Cl, 5 mM EDTA, 150 mM sodium chloride, and 0.1% sodium dodecyl sulfate (SDS), 0.5% sodium deoxycholate, 1% triton X-100, 50 mM HEPES, 1 mM phenylmethanesulfonyl fluoride, and 1 × protease inhibitor cocktail. The extracted proteins were quantified by the Folin-Lowry method and further used for biochemical assays. Superoxide dismutase (SOD), catalase (CAT), glutathione peroxidase (GPx), and glutathione reductase (GR) levels were determined by the previously described methods.[26-29]

Comet assay

HDF cells (1×10^6) were seeded in 6 well plates and treated with FE fraction and silymarin followed by UV-B irradiation. Cells were incubated at room temperature for 30 min. The assay was performed by described previously method.[3] 100 comets of each treatment group were observed at ×400 magnification using a fluorescent microscope and analyzed by Casp software version 2.0 (CaspLab.com), percent head DNA was calculated and statistically analyzed.

Ethidium bromide/acridine orange staining

After pretreatment with FE fraction and UV-B treatment, cells were stained using 1:20 diluted mixture of EtBr and AO (100 μg/ml each). Cells were observed under ×400 magnification using a fluorescent microscope.

Quantitation of intracellular reactive oxygen species

After the FE fraction pretreatment and UV-B treatment, cells were washed and resuspended in DPBS. 10 μl of DCFH-DA (1 μM) was added to the cells and incubated for 45 min at 37°C. The ROS-positive cells were then measured in a flow cytometer at 488 nm laser wavelength and 535 nm detection wavelength.

Nrf2 and HO-1 expression by qPCR analysis

Quantitative PCR (qPCR) analysis for Nrf2 and HO-1 was performed using 18S ribosomal ribonucleic acid (rRNA) as an internal control. Total RNA was extracted from the treatment groups using TRI reagent followed by cDNA synthesis using TAKARA Prime Script 1st strand cDNA synthesis kit. SYBR® green real-time PCR master mix was used for the analysis and the primer sequences and the standardized cycling conditions for Nrf2, HO-1, and 18S rRNA are given in Tables 1 and 2, respectively. Results are represented as fold change in expression as compared to the UV-B control group.

Western blot analysis

Cell lysates were prepared and quantified as mentioned earlier. They were resolved and transferred on nitrocellulose membrane. For Nrf2, the membrane was blocked using 5% bovine serum albumin (BSA) and probed by 1:1000 diluted monoclonal Nrf2 antibody followed by incubation with 1:2000 diluted goat anti-mouse HRP-conjugated secondary antibody. The membrane was incubated with ECL substrate and chemiluminescence was detected on an X-ray film. Membrane was then stripped using stripping buffer (10% SDS, 0.5M Tris-Cl, β-mercaptoethanol) at 55°C for 30 min and washed 5 times using phosphate buffered saline with 0.1% tween 20. The membrane was blocked using 5% BSA and reprobed using 1:500 diluted monoclonal HO-1 antibody followed by the above given procedure. The blot was again stripped and reprobed for β-actin using 5% nonfat dry milk as blocking reagent and 1:1000 diluted monoclonal β-actin antibody followed by the above given procedure.

Statistical analysis

Results were analyzed statistically using one-way analysis of variance and Dunnett's post test on GraphPad Prism software, (GraphPad software, Inc.), ***$P < 0.001$. Unpaired t-test was also used to compare in-between the groups. Results are expressed as a mean ± standard deviation.

RESULTS

TLC, TLC-DPPH and HPTLC analysis

Qualitative separation of bioactive flavonoids from crude alcoholic extract and FE fraction was done by TLC using quercetin, kaempferol, and gallic acid as standards. In Figure 1a and b, lane 1–5 illustrated the bands of quercetin, kaempferol, gallic acid, crude alcoholic extract, and FE fraction,

Table 1: Primer sequences and product sizes of Nrf2, HO-1 and 18S rRNA for real-time PCR analysis

Gene	Primer sequence	Product size (bp)
Nrf2	FP: 5'-GGCTACGTTTCAGTCACTTG-3'	180
	RP: 5'-AACTCAGGAATGGATAATAG-3'	
HO-1	FP: 5'-GAGGAGTTGCAGGAGCTGCT-3'	180
	RP: 5'-GAGTGTAAGGACCCATCGGA-3'	
18S rRNA	FP: 5'-GAGTGTAAGGACCCATCGGA-3'	171
	RP: 5'-CCTCCAATGGATCCTCGTTA-3'	

PCR: Polymerase chain reaction; rRNA: Ribosomal ribonucleic acid; HO-1: Heme oxygenase-1; Nrf2: Nuclear factor E2-related factor 2

Table 2: Standardized cycling conditions for Nrf2, HO-1 and 18S rRNA for real-time PCR analysis

	Nrf2	HO-1	18S rRNA
Initial denaturation	94°C, 5 min	94°C, 3 min	94°C, 3 min
Denaturation	94°C, 20 s 35 cycles	94°C, 20 s 40 cycles	94°C, 30 s 30 cycles
Annealing	57°C, 20 s 35 cycles	70°C, 20 s 40 cycles	60°C, 30 s 30 cycles
Extension	72°C, 20 s 35 cycles	72°C, 20 s 40 cycles	72°C, 30 s 30 cycles
Final extension	72°C, 7 min	72°C, 7 min	72°C, 5 min

PCR: Polymerase chain reaction; rRNA: Ribosomal ribonucleic acid; HO-1: Heme oxygenase-1; Nrf2: Nuclear factor E2-related factor 2

respectively. All the 3 standards were present in the crude and FE fraction. FE fraction indicated the presence of all the flavonoid bands seen in the crude alcoholic extract indicating a successful separation. The bands in lane 5 were more intense showing enrichment of flavonoids during separation. TLC-DPPH analysis is a qualitative test to detect antioxidant potential which showed that increased antioxidant activity in FE fraction may be due to the enrichment of flavonoids. Figure 1c and d exhibited the HPTLC profile and HPTLC spectra of FE fraction. 9 peaks were detected in the HPTLC spectra with their area, area (%), and Rf values given in Table 3. Out of the 9 peaks detected in the HPTLC analysis, peak 7, 8, and 9 were identified as gallic acid, quercetin, and kaempferol, respectively.

Flavonoid content and anti-oxidant activity

The flavonoid content and antioxidant activity of the FE fraction was estimated and compared to the crude alcoholic extract[17] as seen in Table 4. The flavonoid content and antioxidant potential of FE fraction was seen to be higher than the crude alcoholic extract confirming a successful enrichment of flavonoids.

FE fraction exhibited a better antioxidant potential and flavonoid content than alcoholic extract, hence, was studied for UV-B protective effect on HDF cells.

Cytoprotection by MTT assay

Results in Figure 2 indicate that UV-B irradiation significantly reduces the cell viability, whereas, pretreatment of cells with the FE fraction retained the cell viability significantly. Statistical analysis showed that cell viability increased from concentration of 10 µg/ml to 40 µg/ml ($***P < 0.001$). Results demonstrate that FE fraction reduces cell injury and also protects against UV-B induced damage.

Estimation of endogenous antioxidants

Results indicated that the levels of all the four enzymes (SOD, CAT, GPx, and GR) were significantly reduced due to UV-B induced oxidative stress. Pretreatment of cells with the FE fraction retained the levels of all the enzymes significantly ($***P < 0.001$) in a concentration dependent manner from 10 µg/ml to 40 µg/ml indicating a protective effect through the endogenous enzymatic antioxidant system [Figure 3].
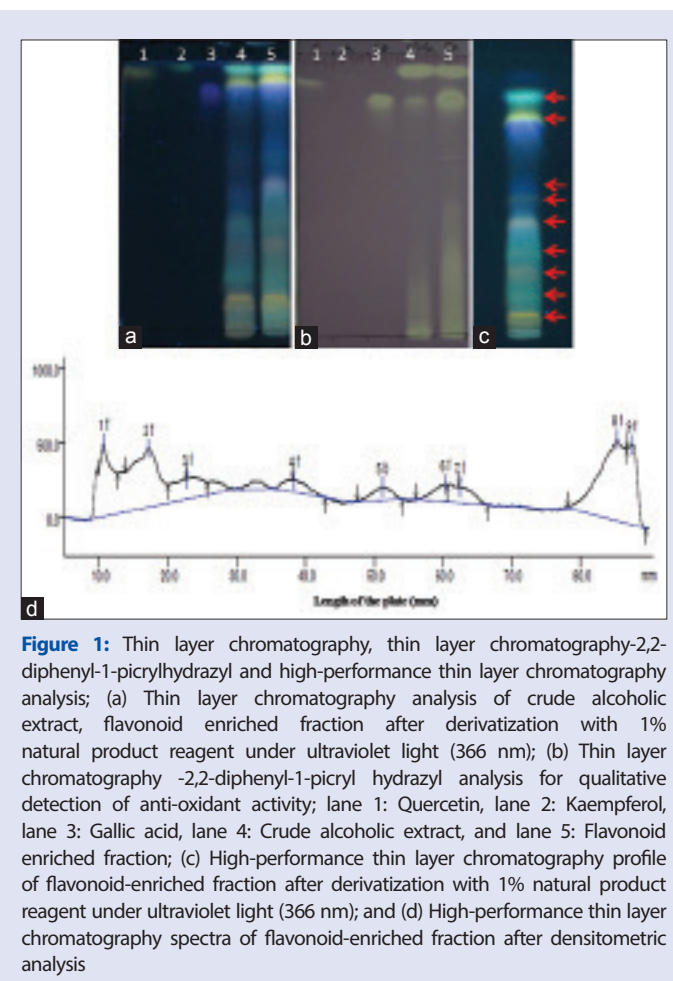

Figure 1: Thin layer chromatography, thin layer chromatography-2,2-diphenyl-1-picrylhydrazyl and high-performance thin layer chromatography analysis; (a) Thin layer chromatography analysis of crude alcoholic extract, flavonoid enriched fraction after derivatization with 1% natural product reagent under ultraviolet light (366 nm); (b) Thin layer chromatography -2,2-diphenyl-1-picryl hydrazyl analysis for qualitative detection of anti-oxidant activity; lane 1: Quercetin, lane 2: Kaempferol, lane 3: Gallic acid, lane 4: Crude alcoholic extract, and lane 5: Flavonoid enriched fraction; (c) High-performance thin layer chromatography profile of flavonoid-enriched fraction after derivatization with 1% natural product reagent under ultraviolet light (366 nm); and (d) High-performance thin layer chromatography spectra of flavonoid-enriched fraction after densitometric analysis

Comet assay

Figure 4 shows results for comet assay done to evaluate the protective effect of FE fraction against UV-B-induced DNA damage. Exposure to UV-B radiations leads to loss of membrane integrity, hence, the fragmented DNA resolved outside the cell as a comet. The UV-B control group showed the least % head DNA indicating a loss of cell membrane integrity and DNA damage. Pretreatment with FE fraction showed a higher % head DNA as compared to UV-B control group indicating protection from UV-B induced DNA damage in a concentration dependent manner ($***P < 0.001$).

Ethidium bromide/acridine orange staining

Results in Figure 5 indicated that UV-B irradiation induced apoptosis and loss of cell membrane integrity as cells appear orange in the UV-B control group. Pretreatment of cells with the lowest concentration of FE fraction (10 µg/ml) illustrated presence of bright spots inside the cell indicating nuclear fragmentation and chromatin condensation, whereas, a concentration of 40 µg/ml showed absence of bright spots in the cell. Results demonstrated protection against apoptotic morphological changes in a concentration-dependent manner as well as the restoration of cell membrane integrity.

Quantification of intracellular reactive oxygen species

Results demonstrated that the UV-B control group showed the significantly higher percentage of ROS-positive cells indicating UV-B-induced formation of ROS. Pretreatment of cells with the

Table 3: Area (%), Rf values and identified components of the peaks detected in the HPTLC spectra after densitometric analysis

Peak	Area	Area (%)	Rf values	Identified components
1	991.98	13.6	0.06	Unknown
2	1789.59	24.5	0.13	Unknown
3	353.22	4.8	0.19	Unknown
4	213.06	2.9	0.37	Unknown
5	294.85	4.0	0.51	Unknown
6	257.40	3.5	0.61	Unknown
7	249.33	3.4	0.63	Gallic acid
8	2337.54	32.0	0.89	Quercetin
9	621.11	11.2	0.91	Kaempferol

Rf: Retention factor; HPTLC: High-performance thin layer chromatography

Table 4: Flavonoid content and EC_{50} values of extracts in DPPH, ABTS and FRAP assays

	Flavonoid content (mg quercetin equivalent/gm plant material)	EC_{50} (µg/ml)		
		DPPH assay	ABTS assay	FRAP assay
Crude alcoholic extract	1.8661±0.0135	16.03±0.84	191.17±3.33	137.80±6.36
FE fraction	3.05±0.07	9.61±0.81	72.48±4.42	118.16±2.52

All values are expressed as mean±SD for 9 experiments.[17] DPPH: 2,2-diphenyl-1-picrylhydrazyl; ABTS: 2,2'-azino-bis-(3-ethylbenzothiazoline-6-sulphonic acid); FRAP: Ferric reducing antioxidant power; EC_{50}: Effective concentration; SD: Standard deviation; FE fraction: Flavonoid enriched fraction

FE fraction showed a significant reduction of ROS-positive cells (***$P < 0.001$) in a concentration-dependent manner from 10 µg/ml to 40 µg/ml as compared to the UV-B control group [Figure 6]. Free radical scavenging property of FE fraction was confirmed through these results.

Nrf2 and HO-1 expression by qPCR analysis

The qPCR analysis was done to evaluate the expression of Nrf2 and HO-1 due to UV-B irradiation. In case of Nrf2, 1.8 fold increased expression was observed in the UV-B control group, whereas, 3.3 fold increase was observed in the case of HO-1 [Figure 7]. Pretreatment of cells with the FE fraction exhibited a significant decrease (***$P < 0.001$) in the expression of both Nrf2 and HO-1 indicating a protective effect through the Nrf2-ARE pathway. The cells in the FE fraction control group showed an increase in the expression of Nrf2 and HO-1 suggesting that the FE fraction induced the antioxidant enzymes without true oxidative stress.

Western blotting analysis for Nrf2 and HO-1

Expression of Nrf2 and HO-1 was determined at the protein level by western blotting analysis using β-actin as an internal control [Figure 8]. UV-B control group indicated overexpression of Nrf2 and HO-1, which may be due to UV-B induced oxidative stress. Pretreatment of the cells with FE fraction indicated a significant concentration-dependent decrease (***$P < 0.001$) in the expression of Nrf2 and HO-1 indicating a protective effect of the FE fraction against UV-B radiation.

DISCUSSION

UV-B radiation is a minor component of the solar spectrum reaching the Earth but is most effective in causing sunburns, aging, immune reactions, and skin cancer. It reacts with photosensitizers and leads to the formation of free radicals[3] which cause various systemic diseases.[30] DNA can absorb UV-B directly leading to the formation of DNA strand
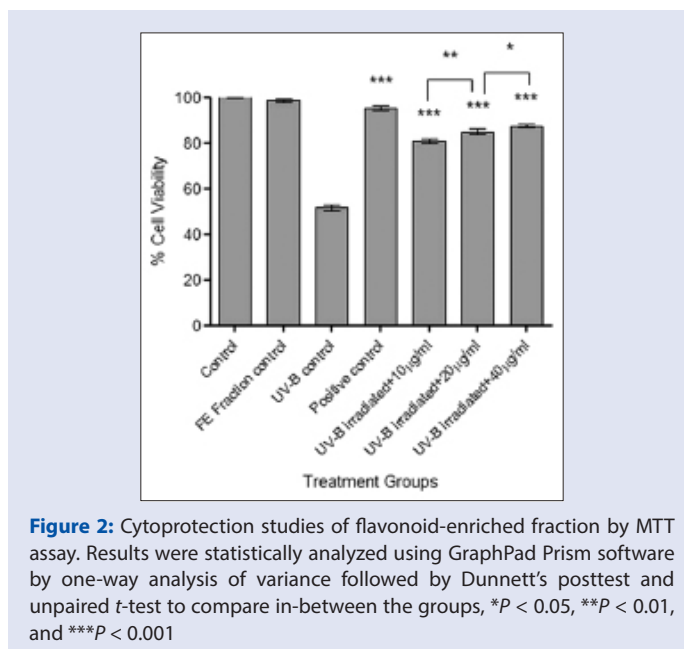

Figure 2: Cytoprotection studies of flavonoid-enriched fraction by MTT assay. Results were statistically analyzed using GraphPad Prism software by one-way analysis of variance followed by Dunnett's posttest and unpaired *t*-test to compare in-between the groups, *$P < 0.05$, **$P < 0.01$, and ***$P < 0.001$

breaks, thymine glycols and 8-hydroxyguanine.[31] Hence, protection from UV-B radiations is very necessary.

Sunscreens and synthetic antioxidants are used as UV protectants but have few limitations on continual use. Chemicals in sunscreens such as zinc oxide and titanium dioxide are unstable, and themselves become free radicals on continuous exposure to UV-B radiations[32] and they can also prevent production of Vitamin D. Some of the natural plant compounds extensively studied for photoprotection are silymarin,[13] sesamol,[3] ursolic acid,[14] ferulic acid,[15] and epicatechin gallate[16] which have successfully attenuated the UV-B induced cytotoxicity, antioxidant depletion, ROS generation, DNA damage, apoptotic morphological changes, etc.

Flavonoids, a type of polyphenols possess good antioxidant potential. FE fraction of clove showed significant flavonoid content and antioxidant potential, hence, was studied further for its photoprotective ability. The FE fraction contains a free radical scavenging ability and also a reducing potential as seen in DPPH, ABTS, and FRAP assays, respectively. Antioxidant ability of flavonoids depends on the structure and substitution pattern of hydroxyl groups, that is, 3', 4'-orthodihydroxy configuration in B ring and 4-carbonyl group in C ring and also the presence of 3-hydroxyl ions (OH) or 5-OH group is essential.[10] Quercetin and kaempferol identified in the FE fraction contain similar configuration along with other unidentified flavonoids can be the reason for a strong antioxidant potential.

UV-B radiation induces intracellular ROS generation in HDF, which is well documented in the literature.[3,13-16] Interaction of UV-B radiations with the cellular chromophores and photosensitizers leads to the formation of ROS and damage to the various bio-molecules such as lipids, proteins, and DNA. In the current study, pretreatment of cells with FE fraction significantly reduced the formation of ROS which reflects the free radical scavenging property of FE fraction.

The endogenous antioxidant system protects against oxidative damage and comprises various enzymes such as SOD, CAT, GPx, and GR and other nonenzymes like bilirubin, uric acid, etc., SOD converts superoxide anion to hydrogen peroxide which is neutralized by CAT to water and oxygen. GPx and GR are involved in removing peroxide and maintaining the oxido-redox status of the cell. GPx and GR maintain the ratio of
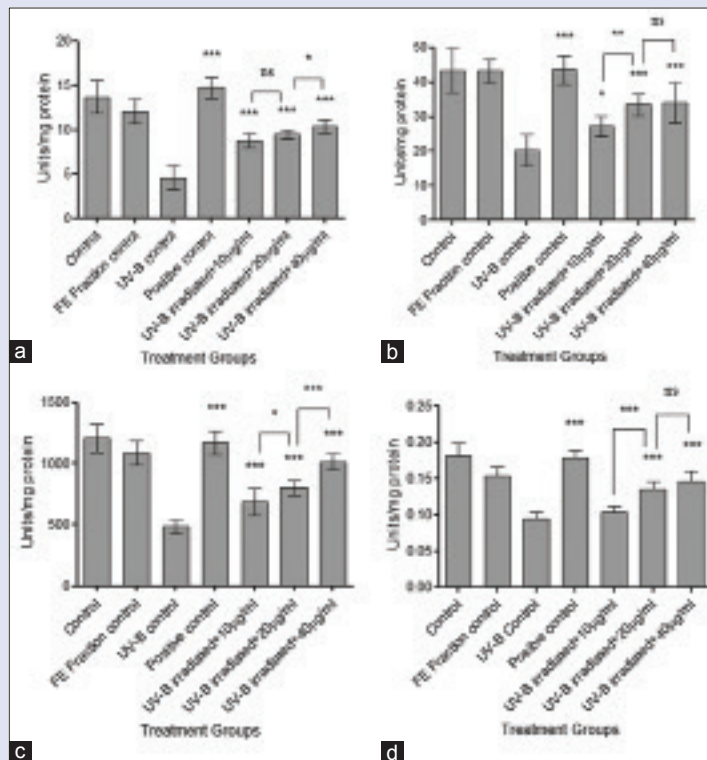
Figure 3: Estimation of levels of endogenous enzymes. (a) Superoxide dismutase; (b) Catalase; (c) Glutathione peroxidase; and (d) Glutathione reductase. Results were statistically analyzed using GraphPad Prism software by one-way analysis of variance followed by Dunnett's posttest and unpaired t-test to compare in-between the groups, $*P < 0.05$, $**P < 0.01$, and $***P < 0.001$
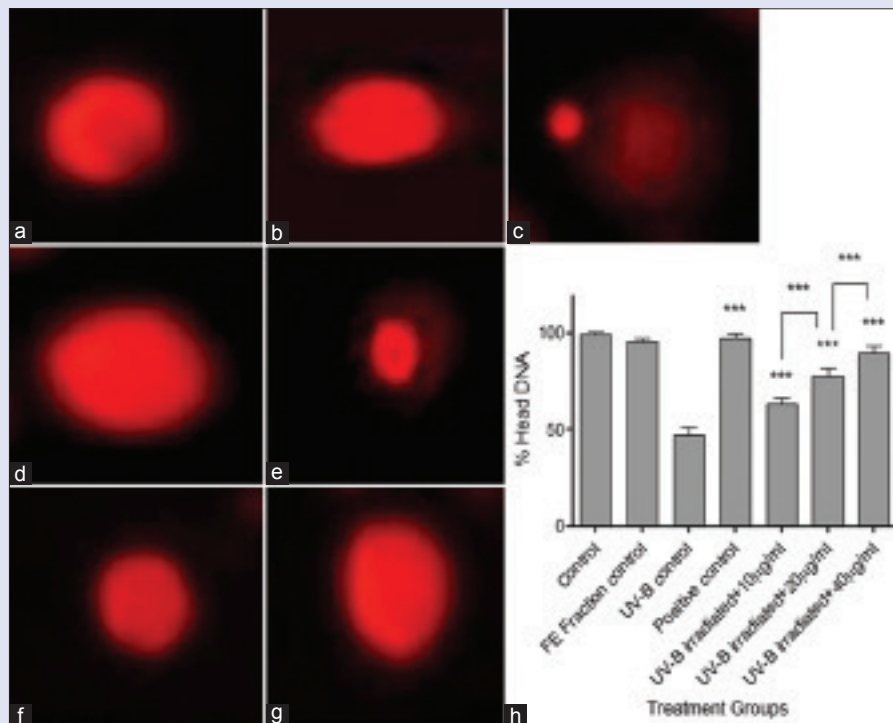

Figure 4: Cells at ×400 in fluorescence microscope and % head deoxyribonucleic acid in treatment groups after alkaline single cell gel electrophoresis. (a) Control; (b) flavonoid-enriched fraction control; (c) ultraviolet-B control; (d) positive control; (e) ultraviolet-B- irradiated fibroblasts + 10 μg/ml fraction; (f) ultraviolet-B-irradiated fibroblasts + 20 μg/ml fraction; (g) ultraviolet-B-irradiated fibroblasts + 40 μg/ml fraction; and (h) comparative graph showing % head deoxyribonucleic acid in all treatment groups. Results were statistically analyzed using GraphPad Prism software by one-way analysis of variance followed by Dunnett's posttest and unpaired t-test to compare in-between the groups, $***P < 0.001$
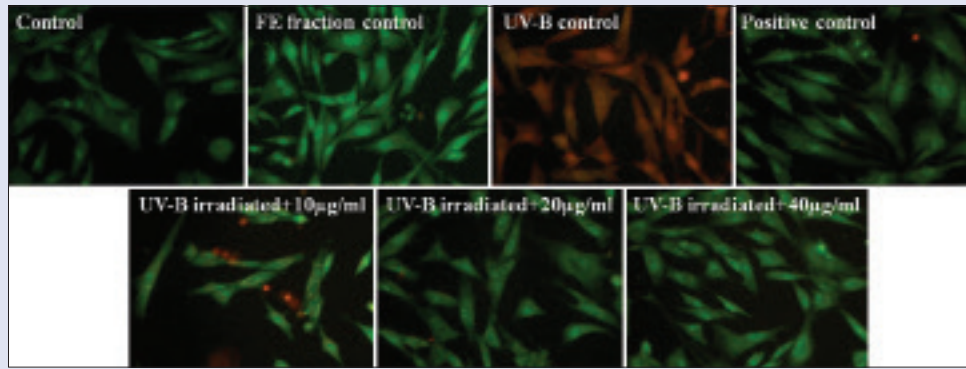
Figure 5: Ethidium bromide/Acridine orange staining. Cells observed under fluorescent microscope, ×400 magnification
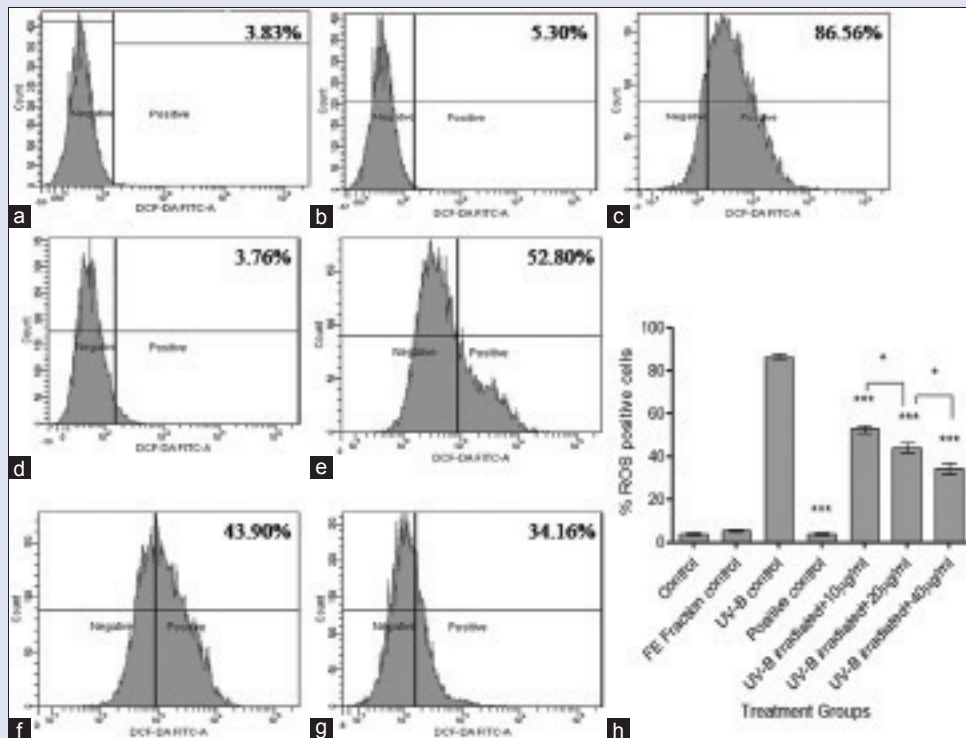

Figure 6: Determination of intracellular reactive oxygen species by 2′,7′-dichlorofluorescein diacetate dye. (a) Control; (b) Flavonoid-enriched fraction control; (c) Ultraviolet-B control; (d) Positive control; (e) Ultraviolet-B-irradiated fibroblasts + 10 μg/ml fraction; (f) Ultraviolet – B-irradiated fibroblasts + 20 μg/ml fraction; (g) Ultraviolet-B-irradiated fibroblasts + 40 μg/ml fraction; and (h) Comparative graph showing % reactive oxygen species positive cells in treatment groups. Results were statistically analyzed using GraphPad Prism software by one-way analysis of variance followed by Dunnett's posttest and unpaired *t*-test to compare in-between the groups, *P < 0.05, ***P < 0.001

GSH/oxidized glutathione which is an important index of oxidative stress and cellular homeostasis.[33] In the current study, UV-B-induced ROS generation may have depleted the levels of endogenous antioxidant enzymes. The antioxidant enzymes are affected due to the direct absorbance of UV-B radiation, interaction with ROS or the antioxidant recycling mechanisms. Heme group absorbs UV-B radiations and decreases CAT activity; depleted SOD may be due to the formation of superoxide anion, and antioxidant recycling mechanism may be the reason for decreased GPx and GR activities.[34] Pretreatment of cells with FE fraction retained the levels of endogenous antioxidant enzymes significantly with a decrease in the levels of ROS. The FE fraction may be useful against diseases caused due to UV-B-induced oxidative stress.

UV-B-induced DNA damage was also observed in HDFs. Oxidative stress-induced DNA damage may be due to the direct absorption of UV-B by DNA or through the formation of ROS.[35] FE fraction pretreatment significantly reduced the DNA damage as seen in comet assay which may be due to the sunscreen effect exerted on DNA. Protective effect of FE fraction on UV-B induced apoptotic changes was studied by EtBr/AO staining. Control cells had intact nuclei, and no changes were seen in the morphology. UV-B radiation lead to apoptotic morphological changes hence showed bright orange cells. Pretreatment with FE fraction reduced the apoptotic morphological changes in the cells showing protection.

The Nrf2-ARE pathway is important in cellular defence. Pretreatment of cells with the FE fraction reversed the UV-B induced overexpression of Nrf2 and HO-1 significantly indicating a protective effect. FE fraction group also showed an increase in expression of Nrf2 and HO-1 without
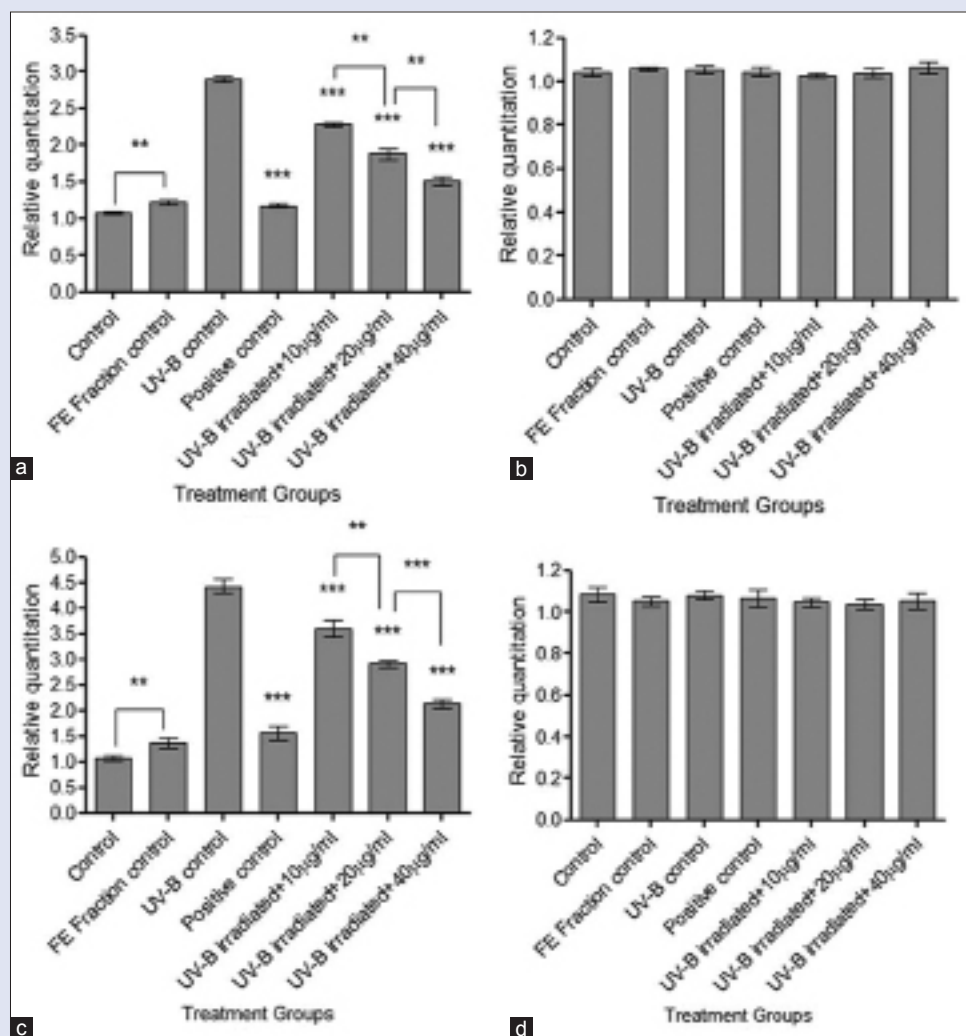
Figure 7: Real-time polymerase chain reaction analysis for nuclear factor E2-related factor 2 and heme oxygenase-1. (a) Fold change in nuclear factor E2-related factor 2 gene expression; (b) Expression of internal control 18S rRNA for nuclear factor E2-related factor 2; (c) Fold change in heme oxygenase-1 gene expression; and (d) Expression of internal control 18S rRNA for heme oxygenase-1. Results were statistically analyzed using GraphPad Prism software by one-way analysis of variance followed by Dunnett's posttest and unpaired t-test to compare in-between the groups, **$P < 0.01$, ***$P < 0.001$

true oxidative stress. The diet-derived phytochemicals are Michael acceptors or are metabolized as such in the body which change the structural conformation of Keap-1 by reacting with its sensor thiols and converting them into thiolates. Hence, the level of unbound Nrf2 in the cytosol increases leading to higher translocation in the nucleus and overexpression of downstream genes which increases the threshold of oxidative stress in the cell. This phenomenon is called as priming of the cell.[36,37] Curcumin and caffeic acid phenethyl ester have shown to stimulate ARE-binding activity of Nrf2 in NRK cells and LLC-PK1 cells along with an increase in the HO-1 activity.[38] Sulforaphane, quercetin,[7] resveratrol, Vitamin E,[39] and peanut sprout extract[40] have also shown overexpression of Nrf2 and its downstream genes. FE fraction not only showed UV-B protection through the Nrf2-ARE pathway but also increased oxidative stress tolerance of the cell.

In the present study, we observed that the FE fraction of clove protected the cells against UV-B-induced cytotoxicity, antioxidant depletion, intracellular ROS, oxidative DNA damage, apoptotic changes, and also protected through the Nrf2-ARE pathway. Taken together, these findings suggest that the flavonoids from clove could potentially be considered as UV-B protectants and can be explored further for its topical application to the area of skin requiring protection.

CONCLUSION

FE fraction of clove exhibited a significant antioxidant and photoprotective ability by reversing UV-B induced cytotoxicity, antioxidant depletion, intracellular ROS, oxidative DNA damage, apoptotic changes and overexpression of Nrf2 and HO-1 genes. Our studies demonstrated for the first time that the FE fraction from clove could confer UV-B protection probably through the Nrf2-ARE pathway. FE fraction also indicated a priming effect on the cells by increasing tolerance of the cell against oxidative stress. The flavonoids from clove have a potential as UV-B protectants and can be explored in the therapeutic and cosmetic market.
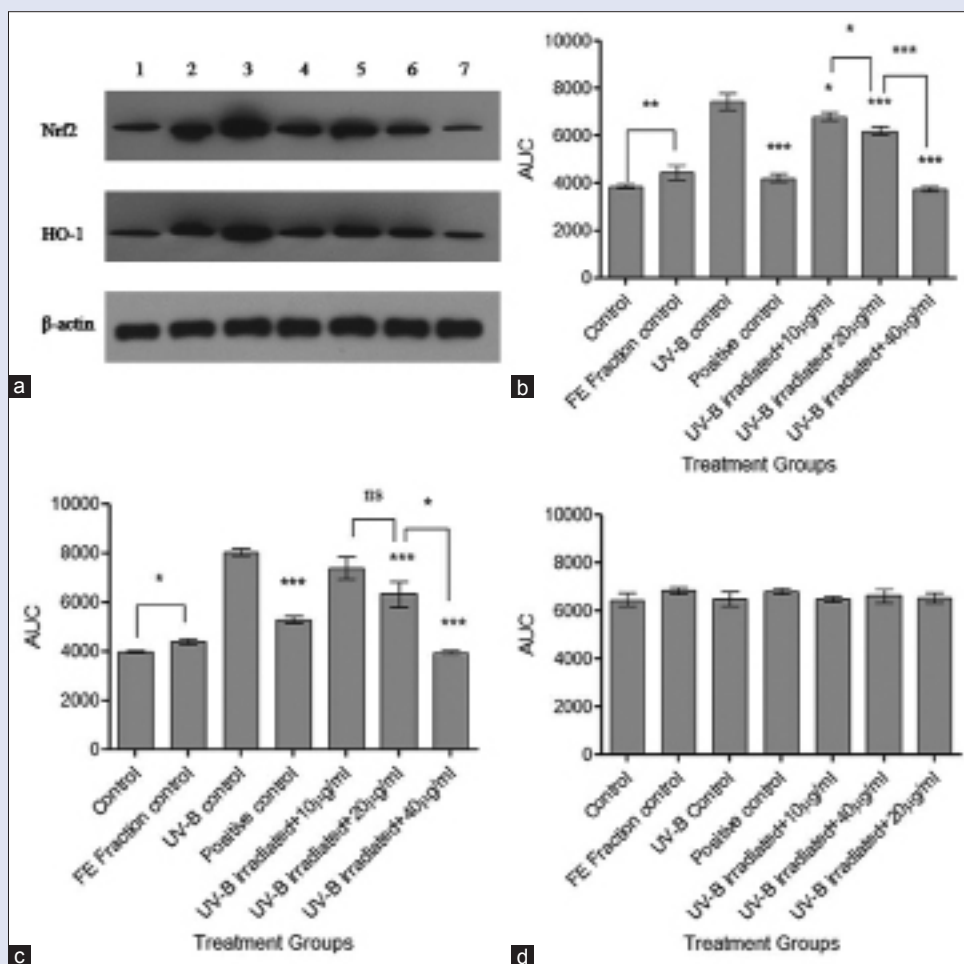
Acknowledgments

Figure 8: Western blot analysis for nuclear factor E2-related factor 2 and heme oxygenase-1. (a) Nuclear factor E2-related factor 2, heme oxygenase-1 and β-actin expression where 1 - control, 2 - flavonoid-enriched fraction control, 3 - ultraviolet-B control, 4 - positive control, 5 - ultraviolet-B irradiated fibroblasts + 10 µg/ml fraction, 6 - ultraviolet-B irradiated fibroblasts + 20 µg/ml fraction, and 7 - ultraviolet-B irradiated fibroblasts + 40 µg/ml fraction; (b) Densitometric analysis of nuclear factor E2-related factor 2 bands; (c) Densitometric analysis of haem oxygenase-1 bands; and (d) Densitometric analysis of β-actin bands. Results were statistically analyzed using GraphPad Prism software by one-way analysis of variance followed by Dunnett's posttest and unpaired t-test to compare in-between the groups, $*P < 0.05$, $**P < 0.01$, $***P < 0.001$

and Miss. Madhura Joshi, IIT Bombay for providing flow cytometer facilities. Authors are thankful to Dr. Nancy Pandita, Dr. Krutika Desai, and Dr. R. Joshi for their critical inputs during the study, and to Dr. Aparna Khanna, Dean, SDSOS, Mumbai for providing facilities for the experimental work.

Conflicts of interest
There are no conflicts of interest.

REFERENCES

1. Afaq F, Adhami VM, Ahmad N, Mukhtar H. Botanical antioxidants for chemoprevention of photocarcinogenesis. Front Biosci 2002;7:d784-92.

2. Katiyar SK. Grape seed proanthocyanidines and skin cancer prevention: Inhibition of oxidative stress and protection of immune system. Mol Nutr Food Res 2008;52 Suppl 1:S71-6.

3. Ramachandran S, Rajendra Prasad N, Karthikeyan S. Sesamol inhibits UVB-induced ROS generation and subsequent oxidative damage in cultured human skin dermal fibroblasts. Arch Dermatol Res 2010;302:733-44.

4. Pinnell SR. Cutaneous photodamage, oxidative stress, and topical antioxidant protection. J Am Acad Dermatol 2003;48:1-19.

5. Black HS, deGruijl FR, Forbes PD, Cleaver JE, Ananthaswamy HN, deFabo EC, et al. Photocarcinogenesis: An overview. J Photochem Photobiol B 1997;40:29-47.

6. Ma Q, He X. Molecular basis of electrophilic and oxidative defense: Promises and perils of Nrf2. Pharmacol Rev 2012;64:1055-81.

7. Alrawaiq N, Abdullah A. Dietary phytochemicals activate the redox-sensitive transcription factor Nrf2. Int J Pharm Pharm Sci 2014;6:11-6.

8. Lee JM, Johnson JA. An important role of Nrf2-ARE pathway in the cellular defense mechanism. J Biochem Mol Biol 2004;37:139-43.

9. Gulcin I, Gungor I, Beydemir U, Elmasta M, Kufrevio I. Comparison of anti-oxidant activity of clove (*Eugenia caryophylata* Thunb) buds and lavender (*Lavandula stoechas* L.). Food Chem 2004;87:393-400.

10. Wojdyla A, Oszmianski J, Czemerys R. Anti-oxidant activity and phenolic compounds in 32 selected herbs. Food Chem 2007;105:940-9.

11. Bhuiyan M, Begum J, Nandi N, Akter F. Constituents of the essential oil from leaves and buds of clove (*Syzygium caryophyllatum* (L.) Alston). Afr J Plant Sci 2010;4:451-4.

12. WHO Monographs on Selected Medicinal Plants.Vol. 2. World Health Organisation; 1999. p. 45-53.

13. Svobodová A, Psotová J, Walterová D. Natural phenolics in the prevention of UV-induced skin damage. A review. Biomed Pap Med Fac Univ Palacky Olomouc Czech Repub 2003;147:137-45.

14. Ramachandran S, Prasad NR. Effect of ursolic acid, a triterpenoid antioxidant, on ultraviolet-B radiation-induced cytotoxicity, lipid peroxidation and DNA damage in human lymphocytes. Chem Biol Interact 2008;176:99-107.

15. Prasad NR, Ramachandran S, Pugalendi KV, Menon VP. Ferulic acid inhibits UV-B – Induced oxidative stress in human lymphocytes. Nutr Res 2007;27:559-64.

16. Huang CC, Wu WB, Fang JY, Chiang HS, Chen SK, Chen BH, et al. (-)-Epicatechin-3-gallate, a green tea polyphenol is a potent agent against UVB-induced damage in HaCaT keratinocytes. Molecules 2007;12:1845-58.

17. Patwardhan J, Pandita N, Bhatt P. Comparative study of anti-oxidant potential of two Indian medicinal plants – Foeniculum vulgare and Eugenia caryophylata. Int J Pharm Sci Rev Res 2013;21:312-6.

18. Lee GS, Shim H, Lee KM, Kim SH, Yim D, Cheong JH, et al. The role of the ethylacetate fraction from hydnocarpi semen in acute inflammation in vitro model. Immune Netw 2012;12:291-5.

19. Wagner H, Bladt S. Plant Drug Analysis – A Thin Layer Chromatography Atlas. 2nd ed. Berlin, Heidelberg: Springer-Verlag; 1996.

20. Sethiya NK, Raja MK, Mishra SH. Antioxidant markers based TLC-DPPH differentiation on four commercialized botanical sources of Shankhpushpi (A Medhya Rasayana): A preliminary assessment. J Adv Pharm Technol Res 2013;4:25-30.

21. Chang CC, Yang MH, Wen HM, Chern JC. Estimation of total flavonoid content in propolis by two complementary colorimetric methods. J Food Drug Anal 2002;10:178-82.

22. Kedare SB, Singh RP. Genesis and development of DPPH method of antioxidant assay. J Food Sci Technol 2011;48:412-22.

23. Re R, Pellegrini N, Proteggente A, Pannala A, Yang M, Rice-Evans C. Antioxidant activity applying an improved ABTS radical cation decolorization assay. Free Radic Biol Med 1999;26:1231-7.

24. Fakruddin M, Mannan KS, Mazumdar RM, Afroz H. Antibacterial, antifungal and antioxidant activities of the ethanol extract of the stem bark of Clausena heptaphylla. BMC Complement Altern Med 2012;12:232.

25. Mosmann T. Rapid colorimetric assay for cellular growth and survival: Application to proliferation and cytotoxicity assays. J Immunol Methods 1983;65:55-63.

26. Marklund S, Marklund G. Involvement of the superoxide anion radical in the autoxidation of pyrogallol and a convenient assay for superoxide dismutase. Eur J Biochem 1974;47:469-74.

27. Chance B, Herbert D. The enzymesubstrate compounds of bacterial catalase and peroxides. Biochem J 1950;46:402-14.

28. Awasthi YC, Beutler E, Srivastava SK. Purification and properties of human erythrocyte glutathione peroxidase. J Biol Chem 1975;250:5144-9.

29. Goldberg DM, Spooner RJ. Oxidoreductases acting on groups other than CHOH glutathione reductase. In: Bergmeyer HU, Bergmeyer J, Grassl M, editors. Methods of Enzymatic Analysis. Weinheim: Verlag Chemie; 1983. p. 258-65.

30. Patlolla A, Knighten B, Tchounwou P. Multi-walled carbon nanotubes induce cytotoxicity, genotoxicity and apoptosis in normal human dermal fibroblast cells. Ethn Dis 2010;20 1 Suppl 1:65-72.

31. Johnson JA, Johnson DA, Kraft AD, Calkins MJ, Jakel RJ, Vargas MR, et al. The Nrf2-ARE pathway: An indicator and modulator of oxidative stress in neurodegeneration. Ann N Y Acad Sci 2008;1147:61-9.

32. Ambothi K, Nagarajan RP. Ferulic acid prevents UV-B radiation induced oxidative damage in human dermal fibroblasts. Int J Nutr Pharmacol Neurol Dis 2014;4:203-13.

33. Rai R, Shanmuga SC, Srinivas C. Update on photoprotection. Indian J Dermatol 2012;57:335-42.

34. Lü JM, Lin PH, Yao Q, Chen C. Chemical and molecular mechanisms of antioxidants: Experimental approaches and model systems. J Cell Mol Med 2010;14:840-60.

35. Shindo Y, Witt E, Han D, Tzeng B, Aziz T, Nguyen L, et al. Recovery of antioxidants and reduction in lipid hydroperoxides in murine epidermis and dermis after acute ultraviolet radiation exposure. Photodermatol Photoimmunol Photomed 1994;10:183-91.

36. Stefanson AL, Bakovic M. Dietary regulation of Keap1/Nrf2/ARE pathway: Focus on plant-derived compounds and trace minerals. Nutrients 2014;6:3777-801.

37. Li W, Kong AN. Molecular mechanisms of Nrf2-mediated antioxidant response. Mol Carcinog 2009;48:91-104.

38. Balogun E, Hoque M, Gong P, Killeen E, Green CJ, Foresti R, et al. Curcumin activates the haem oxygenase-1 gene via regulation of Nrf2 and the antioxidant-responsive element. Biochem J 2003;371(Pt 3):887-95.

39. Atia A, Abdullah A. Modulation of Nrf2/Keap1 pathway by dietary phytochemicals. Int J Res Med Sci 2014;2:375-81.

40. Choi JY, Choi DI, Lee JB, Yun SJ, Lee DH, Eun JB, et al. Ethanol extract of peanut sprout induces Nrf2 activation and expression of antioxidant and detoxifying enzymes in human dermal fibroblasts: Implication for its protection against UVB-irradiated oxidative stress. Photochem Photobiol 2013;89:453-60.

ABOUT AUTHORS

Miss Juilee Patwardhan, is a research scholar at the Department of Biological Sciences, SDSOS, NMIMS, Mumbai under the guidance of Dr. Purvi Bhatt. Her area of research is Phytochemistry, Photoprotection and also studying the effects of ultraviolet radiation.

Dr. Purvi Bhatt, is an Assistant Professor at the Department of Biological Sciences, SDSOS, NMIMS, Mumbai. Her areas of specialization are Biochemistry, Reproductive Biology, and Cancer Biology. She is also actively involved in teaching, training postgraduate students and guiding students for their doctoral research projects in the fields of phytochemistry, cancer biology, and nanotechnology.

Juilee Patwardhan

Purvi Bhatt